

OVERALL CONDITIONS OF YANG YI GEOTHERMAL FIELD

Ejun Xie

The Geothermal Geological Team, Department of Geology and Mineral Resources of Tibet, P. R. China

Key Words: geological, geophysical, geothermal reservoir, characteristics, Yang Yi geothermal field

ABSTRACT

Yang Yi Geothermal Field is located in Dangxiong County, Tibet, about 50 km from Yangbajing Geothermal Field and 75 km from Lhasa. With an average altitude of 4,800 m, it is located in a marsh grassland, semi-drought climatic region of the plateau. The highest and lowest temperatures ever recorded are 21 and -31 °C respectively. The water boiling point under the local atmospheric pressure (0.6 kg/cm²) is 85 °C.

Based on geophysical studies and geothermal reservoir engineering tests, the total area of the geothermal field is estimated to be 10.76 km². It is a tectonic-fissure type high-temperature geothermal field, which is controlled mainly by tectonic fractures stretching from south to north. The highest temperature in the field is 207 °C. The average temperature in the high-temperature region of the geothermal reservoir is 172 °C, and the maximum lip pressure, maximum static pressure and maximum working pressures are 3 kg/cm², 9.4 kg/cm² and 11.3 kg/cm² respectively. The corresponding flow rate for a single well is more than 100 T/h, in terms of total quantity of steam and water.

1. INTRODUCTION

Yang Yi Geothermal Field, located in the Yang Yi sub-basin at the south end of the Yangbajing-Yang Yi basin, which is situated in the east side of the Gandise-Nyainqntaglha connection, has attracted remarkable interest in recent years. The geothermal field is within the Dangxiong-Yangbajing-Duoqinguo active tectonics zone (Fig. 1), belonging to the Mediterranean-Himalayan geothermal belt. The highest and lowest altitudes in the field are 5,050 m and 4,500 m respectively. The climate in the basin is windy and dusty, with low precipitation and long sunshine. Other characteristics of the climate are low temperature, high evaporation, low atmospheric pressure and large diurnal temperature variations.

A detailed survey was carried out during the period of 1985-1990, covering an area of 30 km². Extensive studies have been conducted including surface geology, hydrogeology, geochemistry, geophysics and geothermal drilling. A total of 28 prospecting wells have been drilled with a total drilling depth of 19,063 m (Fig. 2). The depth of each individual well ranges from 312.87 m to 1,149.44 m (Table 1).

2. GEOLOGICAL CHARACTERISTICS

2.1 Strata

The exposed surface layer within the geothermal field is the Cenozoic Neogene system and Quaternary system. The lower bed rock is the early Himalayan acid intrusive rock. The Miocene series (N₁) layer of the upper Tertiary system is the late Himalayan neutral effusive rocks, appearing in the middle

and the west of the field as horsts that become thicker going from the south to north. This layer consists of trachyandensite, trachyte, tuff and pyroclastic rocks, with a total thickness of 521.5 m with the isotopic age of the rocks ranging from 8.64 to 25.3 Ma (K-Ar method). Only a little of the Pliocene series (N₂) layer is exposed on the surface in the north. Consisting of muddy shale, conglomerate and sandy conglomerate rocks, the thickness of the exposed layer is 130.5 m. The lower bed rock, i.e. magmatic rock, is composed of granite porphyry and porphytic granite rocks. The porphytic granite exists as both stock and batholith, which are covered unconformably by the Miocene series volcanic rocks or the lower Pleistocene series clastic rocks. In the western region of the field, the burying-depth is in the range of 50-377.5 m, while in the eastern region, it is in the range of 499.5-686.5 m. On the other hand, the burying depth in the north is shallower than in the south. The isotopic age ranges from 58.5 to 67.7 Ma. The maximum drilling-revealed thickness is 653.5 m (ZK600). The granite porphyry exists as laccolith (either alternating with or covering the porphytic granite), and is also covered unconformably by the Miocene series volcanic rocks or the lower Pleistocene series clastic rocks. The isotopic age of the rock is from 45.05 to 56.2 Ma and the maximum thickness is 599 m as revealed by drilling.

2.2 Fracture Structures

The fracture structures in the field can be classified into three groups: a nearly south-north strike, a north-east to nearly-east-west strike, and a north-west strike. The nearly south-north strike is the main fracture; the other two groups are secondary associated fractures (Fig. 2).

F₁ - F₆ are the nearly south-north faults. The strike of this group of faults is 340-5 °. All the dip angles are above 70 °, except that of F₁ which is 50 °. The vertical off set is about 200 m. The fracture activities of these faults gives rise to the formation of a Miocene series volcanic rock horst (in the middle region of the geothermal field, 7.5 km long, with F₃ and F₅ as the boundaries) as well as fracture subsidence of varied depth along both sides. Among these faults, F₁, F₂ and F₆ are independent faults and moreover, F₆ is a blind fault with a burying-depth of 400-500 m. On the other hand, F₃, F₄ and F₅ are associated or connected with each other. Due to their deep cuts and active motions, they are the main fractures responsible for the hydrothermal activities.

F₇ - F₁₂ are the north-east to nearly east-west faults. The strike is 38-95 ° and dip angles are around 70 °. Although the vertical stratigraphic separation is only a 2-digit value, these faults have deep cuts and active motions. The intersection of faults F₇ - F₁₁ with the previously mentioned group of faults (F₁ - F₆) results in vigorous hydrothermal activities on the surface, forming boiling spouters and a large area of sinter stage.

F₁₃, F₁₄ and F₁₅ are the north-west faults (the strike: 290-310 °). They are not fully matured. However, there are still strong surface geothermal indications at the fault F₁₃. In addition,

F_{15} intersects with F_5 , which alters the direction towards the west.

As mentioned above, F_3 - F_5 , F_7 - F_{11} and F_{13} are not independent individual faults. Instead, they intersect and cut each other, and thus form a south-north strike fracture network. It is along this network that the geothermal fluid moves to the surface and forms the central part of the geothermal field.

3. GEOPHYSICAL CHARACTERISTICS

3.1 Resistivity and Apparent Resistivity of the Rock and the Water

The resistivity of different types of rocks and water in the geothermal field show varied values. The cold water and hot water have large differences in resistivity. This indicates that the temperature and the amount of total dissolved solids significantly influence the resistivity of the water.

The clayey rocks have the lowest resistivity (less than $7 \Omega \cdot m$). While the resistivity of sandy gravels without water is up to $690 \Omega \cdot m$, the water-containing sandy gravels have similar resistivity to the clayey gravels (both around 200 - $250 \Omega \cdot m$). The corresponding values of the volcanic rocks and granite porphyry rocks are in the range of 370 - $550 \Omega \cdot m$, whereas the surface andesite has a value as high as $700 \Omega \cdot m$. However, they are all one magnitude lower than the normal values (andesite: 2×10^4 ; tuff: 2×10^3 ; granite porphyry: 5×10^3), reflecting the fracture and alteration nature of the rocks.

Upon fracture, alteration and saturation with water, the values of the apparent resistivity of different types of rocks decrease remarkably and become identical (the values are usually in the range from several $\Omega \cdot m$ to several ten $\Omega \cdot m$). This fact reduces the capability of the apparent resistivity curve to differentiate the different rock formations. On the other hand, this has made it easier to differentiate and classify the geothermal reservoir layer.

The apparent resistivity of the geothermal reservoir is higher than that of the caprock. This suggests that the body of the geothermal reservoir is mainly the fractured granite zone, whereas the caprock consists primarily of severely altered pyroclastic rocks, granite weathered zone and the low Pleistocene series clay layer.

3.2 Data Analysis

The minimum apparent values ($\rho_{s \min}$) of the resistivity soundings in the geothermal field generally vary from 1.84 to $20 \Omega \cdot m$ (Fig.2). The trend is a gradual decrease moving from the borderline to the volcanic rock horsts in the central region of the field, reaching a minimum value of less than $5 \Omega \cdot m$ at the intersections of F_3 - F_5 with F_7 - F_9 and F_{11} . The $\rho_{s \min}$ equivalent contour where $\rho_{s \min}=10 \Omega \cdot m$ is approximately identical to the highest temperature equivalent line where $T_{\max}=90^{\circ}C$. Based on this, one can find the scope of the high temperature region of the geothermal field. On the other hand, the $\rho_{s \min}$ equivalent line with $\rho_{s \min}=20 \Omega \cdot m$ indicates approximately the area of the low temperature region. However, in both cases, the tongue-shape extensions towards the northwest do not directly reflect the situation of the

geothermal reservoir. They seem to be associated with F_{13} and with the Pliocene series and lower Pleistocene series muddy rocks at those sites.

The apparent resistivity log curves reflect approximately the changes of apparent resistivity in the vertical direction. Generally, the differences in apparent resistivity between different rock layers within the field are not significant, usually about 20 - $30 \Omega \cdot m$. The upper and lower regions display higher apparent resistivity ($>50 \Omega \cdot m$), while in the middle the corresponding value is ca. 20 - $50 \Omega \cdot m$. The relatively high apparent resistivity is a reflection of the electric nature of the sandy gravels (either with water or without water) and the volcanic rocks. The low values ($<20 \Omega \cdot m$) in the middle are in accordance with the electric nature of the lower Pleistocene series clay layer, the altered pyroclastic rock zone under the Miocene series and the weathered zone on the top of the granite rocks, which together form the caprock of the geothermal reservoir. Similarly, the relatively high apparent resistivity in the lower region reflects the nature of the geothermal reservoir within the granite structure fissures. At the south end, the apparent resistivity below ZK100 is found to be above $1,000 \Omega \cdot m$, indicating that this site is already at the edge of the geothermal field.

4. NATURE OF THE GEOTHERMAL RESERVOIR

4.1 Caprock

Based on the information from drilling investigations, the thickness of the caprock within the geothermal field has a maximum value of $625 m$ and a minimum value of $110 m$. The caprock is 200 - $300 m$ thick in the horst region where the temperature is above $150^{\circ}C$. In the medium-temperature (90 - $150^{\circ}C$) region (i.e. the fracture subsidence along both sides of the horst), the caprock is 110 - $555 m$ thick, while in the low temperature region it is 190 - $625 m$ thick. The rock-composition of the caprock is relatively complex. Close to the surface are mainly sandy gravel rocks, loam and clay, below these are trachyte, trachyandensite and tuff.

4.2 Characteristics of the Geothermal Reservoir Layer

None of the 28 prospecting wells within the field has reached the bottom limit of the geothermal reservoir. In these wells the exposed thickness of the geothermal reservoir is between 63 and $763 m$ (high temperature region: 63 - $703 m$; medium temperature region: 159 - $729 m$; low temperature region: 271 - $763 m$). In fact, the situation of the geothermal reservoir is closely associated with the change of the topography and geomorphology. It changes as the surface configuration rises and falls. The main rock-components of the geothermal reservoir layer are granite porphyry and porphyritic granite that have experienced structural fracture and high-temperature alteration, thus with matured fissures.

4.3 Characteristics of the Temperature Field

The data obtained from temperature logging can be classified into three types according to the shapes of the corresponding curves (Fig. 3). In the first type, the temperature increases quite fast (temperature gradient: 47 - $72^{\circ}C/100m$) in the upper part of the curve which corresponds to the temperature-conductive layer, regarded as the caprock of the geothermal reservoir. The curve is relatively flat in the middle and lower

part, exhibiting only small increase (temperature gradient: 5.5 °C/100m). This region corresponds to the convection layer and is considered to be the geothermal reservoir layer. In this case, the temperature in the hole is relatively high, indicating that the hole (such as ZK300, ZK208) is in the center of the geothermal reservoir.

The curve shape of the second type data is similar to the first type except that the lower part of the curve has a reversal, i.e. the temperature goes down. This fact reflects motions of geothermal fluid towards the side directions, suggesting that the hole (such as ZK250) is already at the edge of the geothermal field.

In the third type, the whole curve is fairly flat, with no obvious inflection point. There is no such region where the temperature increases significantly. In fact, the average temperature increase-gradient for the whole hole is only 6.25 °C/100m. In this case, it is meaningless to differentiate the covering layer and the geothermal reservoir layer, since the hole (e.g. ZK100) is already far away from the geothermal reservoir.

The temperature field in the geothermal field is controlled by the fracture structure. Thus the horst region in the middle of the field is divided by F_{10} into two parts, the south and the north (Fig. 2). The temperature in the south region is slightly higher than that in the north. This can be easily understood since the south region has a thicker caprock (ca. 300 m), thus good heat preservation and insulation properties which enable the heat accumulation within the geothermal reservoir (e.g. the hole ZK203: 201 °C; ZK208: 207 °C). On the other hand, the caprock in the north region is thinner (ca. 200 m), causing considerable heat loss (as indicated by surface geothermal manifestations), and resulting in poor heat preservation and therefore lower temperatures (e.g. ZK403: 191 °C). This has been further confirmed in the horizontal temperature contour at different vertical scales (Fig. 4). For example, as shown by the temperature equivalent lines, there are two high temperature centers at the altitude of 4,250 m, the south center and north center (the former centered at 200 °C, the latter at 190 °C), while at the altitude of 4,000 m, the high temperature region is shifted to the south.

4.4 Characteristics of the Pressure Field

The high-pressure center in the geothermal field is at ZK300 which is located within the horst region. The high-pressure region corresponds to the high temperature region in that they both, run south-north and are distributed in a zonal pattern along the F_3 - F_5 fracture zone. This reveals that the geothermal reservoir center is associated with the F_3 - F_5 fracture zone, which was the passageway for the magma eruption in earlier times, and then later, as the crustal movement continued, became the passageway for the geothermal fluid.

The mean pressure gradient in the geothermal field is 0.1 bar/m. Higher pressure-gradients have been found at certain sites, such as ZK200 (0.101 bar/m), ZK203 (0.103 bar/m) and ZK208 (0.110 bar/m). Such abnormal pressure phenomena suggest that these are high-temperature and high yielding wells, which are located in the central region of the geothermal field (Table 1). The fact that ZK300 fails to become a flowing artesian well is mainly due to the high

altitude of the well-opening (4,854.34 m) and the low water-level (96.17 m below the surface) at the site, therefore relatively high pressure of the water column. Should it be at the site of ZK208, it would also become a high-temperature (ZK300: 196.5 °C) and high-yielding well.

4.5 Geothermal Reservoir Engineering Tests

Individual flowing tests have been performed on 7 flowing artesian wells within the geothermal field. Due to the restrictions of the circumstance, no liquid-vapor separator was installed. The calculation of the parameters, such as total quantity of steam and water, were fulfilled using the JAMES Lip Pressure Method and the results are summarized in Table 1. In addition, an interference test on water levels was also carried out, with ZK208 acting as the primary flowing well, the other 6 wells observed for any effect due to the flowing of well ZK208.

5. HYDROTHERMAL SYSTEM

5.1 Chemical Characteristics of the Water

The chemical nature of the cold water within and around the geothermal field is that of a HCO_3 -Ca type. The concentration of total dissolved solids is 0.1 g/L and the pH is 7. The cations are primarily Ca^{2+} and Na^+ , then Mg^{2+} and K^+ . The anions are mainly HCO_3^- , then SO_4^{2-} , Cl^- and CO_3^{2-} . The content of F^- is usually very low, distributed mainly among the hills surrounding the geothermal field.

The chemical nature of the hot water within the geothermal field is of HCO_3 -Na type, with pH=7.5-9.5 and a concentration of total dissolved solids: 0.3-1.8 g/L. The major components are K^+ , Ca^{2+} , Na^+ , Mg^{2+} , Li^+ , Cl^- , SO_4^{2-} , HCO_3^- , CO_3^{2-} , F^- , B and SiO_2 . Fe^{2+} , Fe^{3+} , NH_4^+ , Cu^{2+} , Pb^{2+} , Zn^{2+} , I^- , Br^- , Hg , As , Mo are the trace components found in the hot water. The contents of Li^+ , CO_3^{2-} , F^- , Cl^- , SiO_2 and B in the hot water are several ten to several hundred times higher than in the cold water. The gas components in the hot water include N_2 , CO_2 , O_2 , H_2S , CH_4 , He and H_2 .

5.2 Hydrothermal Circulation System

According to the information from synthetic earthquakes, 6 km below the geothermal field exists a melt and semi-melt rock body, ca. 4 km wide in the east-west direction and 5 km long in south-north direction. This is the source of heat for the geothermal field. As shown in Fig 5, the geothermal fluid is formed as follows: the cold water on the surface gets to the heat source through deep circulation and seepage. After being heated up, it moves up along the faults to the surface and is discharged in all directions as hot springs and boiling spouters.

6. CONCLUSIONS

We have carried out extensive studies to investigate Yang Yi Geothermal Field. Based on the information from temperature, pressure and geothermal reservoir engineering tests, the area of the geothermal is estimated to be 10.76 km² (Fig 4), according to the equivalent lines of minimum apparent resistivity and the characteristics of the geological structures. The geothermal field is divided into three regions (high-temperature, medium-temperature and low-temperature)

according to the temperature. The high-temperature region, with an area of 1.60 km², is located mainly within the F₃-F₅ fracture zone. The drilling wells in this region usually have high flow rates (usually above 100 T/h for a single well, in terms of the total quantity of steam and water) and high temperatures (above 150-200 °C). The medium-temperature region is situated outside the high-temperature region, with an area of 3.23 km², and temperatures in the range 90-150 °C. The drilling wells in this region are primarily flowing wells or geysers with flow rates (total quantity of steam and water for a single well) less than 100 T/h. The low-temperature region is located outside the above two regions. With the equivalent line of $\rho_{s\min}=10 \Omega\cdot m$ as its outer limit, the area of this region is 5.93 km² and the temperatures range from 35-90 °C.

In summary, Yang Yi, following the discovery of Yangbajing Geothermal Field, is another high-temperature geothermal field in China. Over the years, investigations and explorations have provided a clear picture about the nature of the geothermal reservoir and about the distribution of the geothermal field. It is a structure-fissure type high-temperature geothermal field that has tremendous potential for exploitation.

REFERENCES

Reports

1. Tingli Liang, Ejun Xie, et al. 1989. Exploration Report of the Yang Yi Geothermal Field of Dang Xiong County of Tibet Autonomous Region. pp19-98
2. Degeng Cai et al. 1988. Geological Detailed Survey Report of the Yang Yi Geothermal Field of Dang Xiong County of Tibet Autonomous Region. pp15-20
3. Zixiao Lei, et al. 1989. Geophysical prospecting Survey Report of the Yang Yi Geothermal Field of Dang Xiong County of Tibet Autonomous Region. pp25-45
4. Ligong Zhou, et al. 1982. Synthetic Earthquake Exploration. Report of the Yang Yi Geothermal Field of Dang Xiong County of Tibet Autonomous Region. pp75

Books

5. L.M. Edwards, etc. 1982. Geothermal Energy Manual.
6. Geological dictionary office 1978. Geological Dictionary.

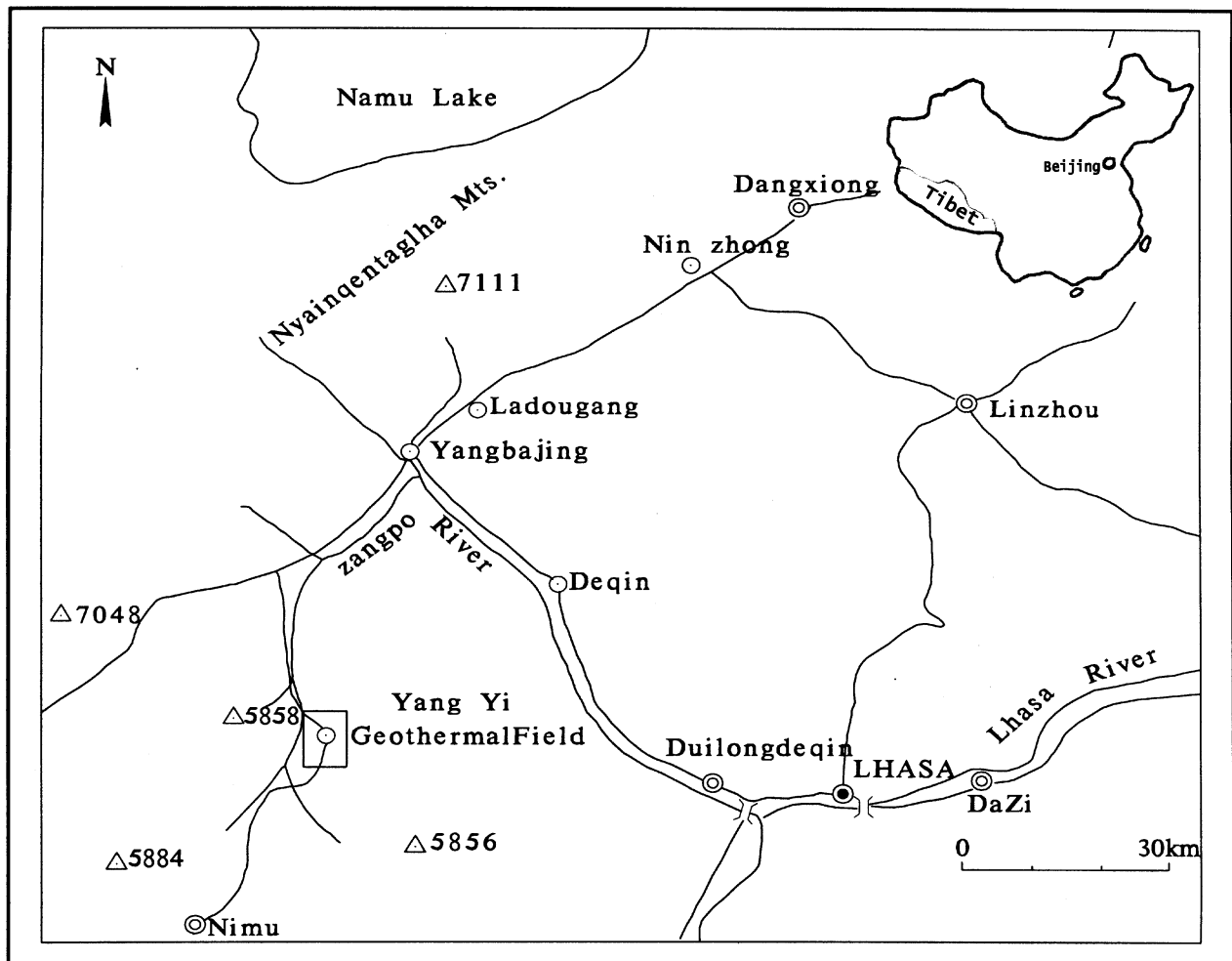
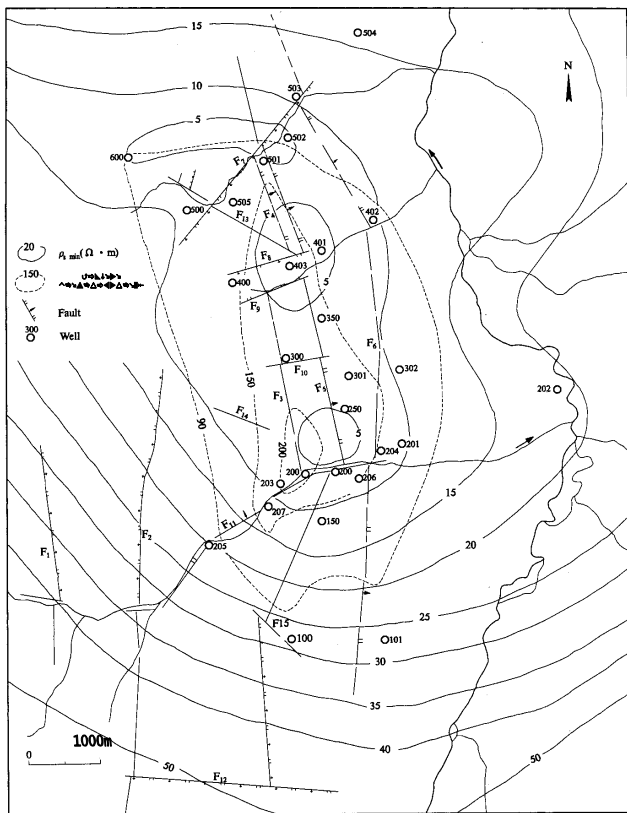


Figure 1. Location Map of Yang Yi Geothermal Field

Table 1. Well data of Yang Yi Geothermal Field

Well type	Flowing artesian well	Geysirine well	Flowing well	Other	Well depth (m)	Total depth (m)	Static temperature of well head (°C)	Working temperature of well head (°C)	Maximum temperature of well head (°C)	Static pressure of well head (kg/cm²)	Working pressure of well head (kg/cm²)	Lip pressure (kg/cm²)	I.D of discharge pipe (cm)	Total quantity of steam and water (t/h)	Steam quantity (t/h)	Ratio of steam to water (%)	Dryness fraction (%)	Elevation of well head (m)	Water level (m)
					zk200	606.22	61.4	134.0	172.39	9.4	3.2	1.1	15.7	95.00	16.0	20.0	17.0	4638.21	4729.25
					zk203	386.00	85.4	166.0	201.77	8.3	9.1	3.4	15.7	236.00	59.0	33.4	25.0	4657.10	4738.99
					zk206	953.00	41.7	105.0	152.34	9.6	1.55		15.7	26.61	3.46	14.9	13.0	4619.04	4711.57
					zk208	312.87	20.0	190.0	207.16	10.0	11.9	3.6	19.7	381.00	102.4	36.8	26.9	4641.34	4738.99
					zk301	439.36	116.0	130.1	165.26	5.7	3.1	0.8	8.0	18.41	3.0	19.0	16.0	4662.27	4715.16
					zk403	789.35		164.0	190.84	3.6	6.2	2.4	15.7	185.00	41.0	28.6	22.2	4710.65	4738.80
					zk501	317.90		108.0	141.00	3.6	1.7			32.18	3.45	12.0	10.7	4686.75	4717.10
					zk207	703.54			163.51	5.9								4666.56	4719.63
					zk401	724.50			136.72	3.0								4675.14	4698.70
					zk101	761.00			65.50	2.65					3.13			4619.80	4641.57
					zk250	724.13			189.93	0.61					0.05			4719.61	4719.71
					zk302	825.50			130.96	2.25					0.70			4578.86	4597.75
					zk402	1149.44			104.00	4.10					0.87			4598.43	4634.13
					zk502	818.00			86.29	0.85					3.28			4675.58	4677.87
					zk100	805.84			66.70									4766.48	4681.89
					zk150	603.88			119.00									4710.57	4649.67
					zk202	403.48												4547.96	4547.96
					zk204	1106.69			144.70									4604.61	
					zk205	600.03			74.00									4704.23	4670.23
					zk300	803.04			196.50									4854.34	4758.17
					zk400	603.00			144.74									4804.81	4735.20
					zk350	902.50			157.27									4734.94	4727.05
					zk500	551.90			120.41									4819.30	4689.30
					zk503	702.26			60.00									4619.90	4585.90
					zk504	605.70			52.00									4565.98	4565.98
					zk505	705.73			132.50									4792.79	4715.39
					zk600	953.00			90.50									4831.02	4691.02
					zk201	253.10												4597.80	



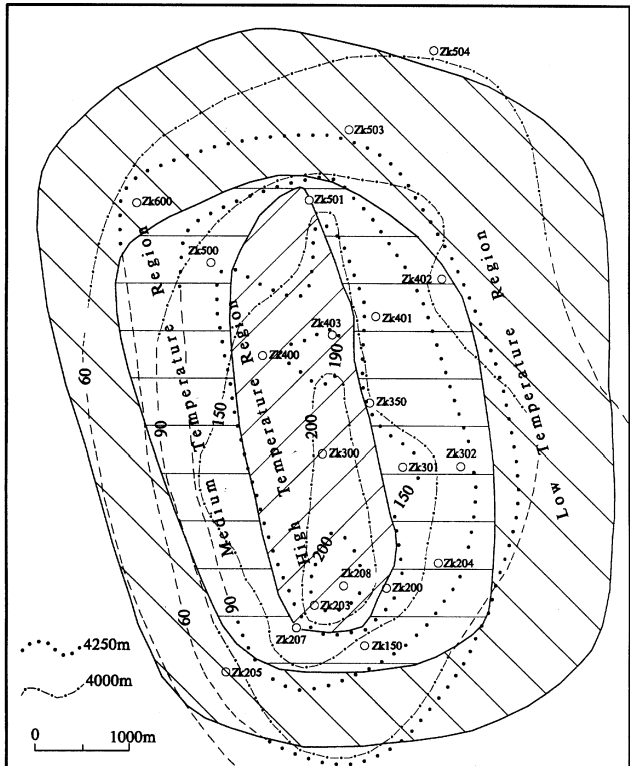


Figure 4. Map of Horizontal Temperature Contour

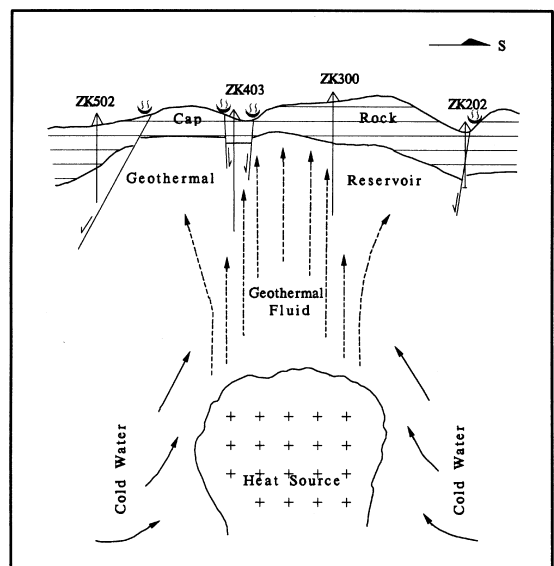


Figure 5. Map of Hydrothermal Circulation System